Selective C−C vs C−H Bond Activation by Rhodium(I) PCP Pincer Complexes. A Computational Study

Andreas Sundermann, Olivier Uzan, David Milstein, and Jan M. L. Martin*

Contribution from the Department of Organic Chemistry, Weizmann Institute of Science, Kimmelman Building, Room 262, IL-76100 Rehovot, Israel

Received March 16, 2000

Abstract: A theoretical study of the oxidative addition of C−C vs C−H bonds to a rhodium(I) complex with PCP-type ligands has been carried out. Special attention has been paid to the effect of different bulky substituents at the phosphorus atoms of the chelate ligand. Therefore, B3LYP/lanl2dz+p//B3LYP/lanl2dz and ONIOM-(B3LYP/lanl2dz+p:B3LYP/lanl2dz)//ONIOM(B3LYP/lanl2dz:HF/lanl1mb) methods have been utilized. According to the calculations, C−H activation is always the kinetically favored process ($\Delta\Delta E^{\ddagger}$ 20 kJ·mol^{-1}), though the C−C activation product is more stable ($\Delta\Delta E$ 20 kJ·mol^{-1}). C−H addition is a reversible process; the product of the C−H activation can interconvert to the C−C activation product via an intermediate structure. Bulky substituents are found to increase the barrier for C−H activation relative to that for C−C activation. With additional ligands (e.g., phosphines), hexacoordinate complexes are formed. This is more favorable for the C−C activation products. Our calculations show that the activation reaction proceeds via complexes with a pentacoordinated rhodium atom. Thus, in the presence of donor ligands, the activation reaction is inhibited.

Introduction

Saturated hydrocarbons containing only C−H and C−C bonds are usually considered to be chemically inert. Using transition metal complexes, activation of these bonds was found to be possible even under mild conditions in solution.[1−8] Theoretical investigations of this important reaction focused on simple model systems such as the oxidative addition to atoms,[9,10] linear d^{10} fragments (e.g., Pt(PH$_3$)$_2$[11]), or T-shaped d^8 fragments (e.g., RhCl(PH$_3$)$_2$[12]). More details about theoretical studies on oxidative additions and reductive eliminations, especially of C−H bonds, can be found in a very recent review by Niu and Hall,[13] so this will not be discussed here in detail.

In most cases, an oxidative addition of the C−H bond to the transition metal center seems to be kinetically and thermodynamically more favorable than C−C activation (selective C−C bond cleavage could be achieved by the use of highly strained substrates such as cyclopropane[14]). A recent review on the experimental aspects has been given by Rybtchinski and Milstein.[15] As a theoretical explanation[10] for the higher activation barrier of C−C bond cleavage, the difference of directionality between a C−C and a C−H bond has been widely accepted. However, Milstein et al. discovered that PCP ligands[5,7,16] (e.g., the ligand 1,3-bis[(di-*tert*-butylphosphino)methyl]-2,4,6-methylbenzene) in combination with rhodium(I) alkene complexes yield a reaction system in which both competing reactions (CC vs CH activation) can be observed simultaneously (see Scheme 1).

For this system, the insertion into the C−H bond is reported to be a reversible process. Thus, the hydride complex ("CH product") **2** can convert into the thermodynamically stable methyl complex ("CC product") **3** under mild conditions, although the observed rate of this conversion is slower than the direct C−C activation. This experimental finding implies the existence of an intermediate structure linking these two products (and the transition states leading to them) on the energy hypersurface. Because of the elusive nature of most of the species involved, the competing activation mechanism of the CH and the CC bonds starting from the joint intermediate is an interesting target for a computational approach. Since it is furthermore known from experiment[15,16] that the feasibility of this reaction (i.e., the height of barriers and the relative energies of the products) is a function of the organic substituents at the phosphorus atoms, we performed calculations on a variety of systems with different substituents at the phosphorus atoms. Specifically, we considered R = hydrogen, methyl, isopropyl, *tert*-butyl, phenyl, and chlorine within this study (although complexes with R = H, Cl are experimentally hitherto unknown). In other words, we tried to model the complete ligand

* Corresponding author. (e-mail) comartin@wicc.weizmann.ac.il.
(1) Bergman, R. G. *Science* **1984**, *223*, 902.
(2) Crabtree, R. H. *Chem. Rev.* **1985**, *85*, 245−269.
(3) Crabtree, R. H. In *The Chemistry of Alkanes and Cycloalkanes*; Patai, S., Rappoport, Z., Eds.; Wiley: New York, 1992.
(4) Burger, P.; Bergman, R. G. *J. Am. Chem. Soc.* **1993**, *115*, 10462−10463.
(5) Gozin, M.; Weisman, A.; Ben-David, Y.; Milstein, D. *Nature* **1993**, *364*, 699−701.
(6) Arndtsen, B. A.; Bergman, R. G.; Mobley, T. A.; Peterson, T. H. *Acc. Chem. Res.* **1995**, *28*, 154−167.
(7) Rybtchinski, B.; Vigalok, A.; Ben-David, Y.; Milstein, D. *J. Am. Chem. Soc.* **1996**, *118*, 12406−12415.
(8) Periana, R. A.; Taube, D. J.; Gamble, S.; Taube, H.; Satoh, T.; Fujii, H. *Science* **1998**, *280*, 560−564.
(9) Low, J. J.; Goddard, W. A., III. *Organometallics* **1986**, *5*, 609−622.
(10) Blomberg, M. R. A.; Siegbahn, P. E. M.; Nagashima, U.; Wennerberg, J. *J. Am. Chem. Soc.* **1991**, *113*, 424−433.
(11) Sakaki, S.; Mizoe, N.; Musashi, Y.; Biswas, B.; Sugimoto, M. *J. Phys. Chem. A* **1998**, *102*, 8027−8036.
(12) Koga, N.; Morokuma, K. *J. Am. Chem. Soc.* **1993**, *115*, 6883−6892.
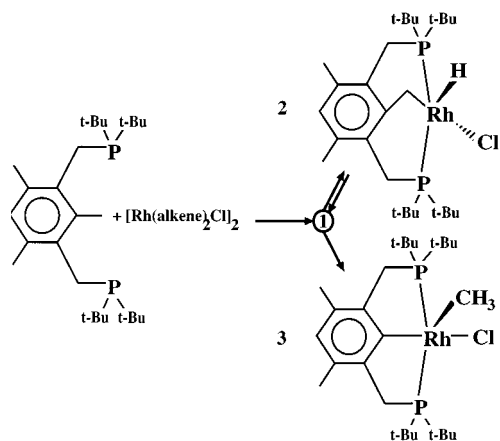(13) Niu, S.; Hall, M. B. *Chem. Rev.* **2000**, *100*, 353−406.

(14) Periana, R. A.; Bergman, R. G. *J. Am. Chem. Soc.* **1986**, *108*, 7346−7355.
(15) Rybtchinski, B.; Milstein, D. *Angew. Chem., Int. Ed.* **1999**, *38*, 871−883.
(16) Liou, S.-Y.; Gozin, M.; Milstein, D. *J. Am. Chem. Soc.* **1995**, *117*, 9774−9775.
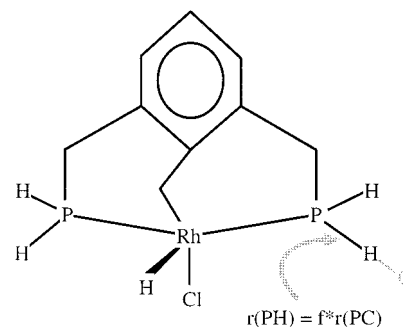
Scheme 1

Figure 1. Graphical representation of the inner layer complex used in the ONIOM calculation. The parameter *f* defines the position of the auxiliary hydrogen atoms.

system used in the experimental study (omitting only the methyl groups in the 4- and 6-positions of the phenyl ring) to uncover those structural features of the ligand which are most important for the reactivity of the transition metal complex. This also includes a study of the effect of an additional ligand because for the PCP ligands with R = methyl (CC product) and phenyl (CH product) the hexacoordinated transition metal complex is obtained.[5,16] PH_3 was used as a model compound for this ligand in our calculations. During the final stage of the preparation of this article we received a preprint of a paper by Cao and Hall[17] dealing with the PCP system. In contrast to this work, we are interested predominantly in substituent effects on the CH and CC activation reaction and not so much in the exploration of the complete energy hypersurface.

Computational Methods

To be able to perform calculations on complexes with large organic substituents, we utilized the ONIOM method developed by Morokuma et al.[18] Within this extrapolation scheme, different parts of the molecule are treated at different levels of theory, according to their relevance for the molecular structure/ properties. For a given nuclear arrangement in a first step the electronic energy of the whole molecule (including all substituents) is calculated at a low level of theory (E_{tot}^{low}). For our calculations, the Hartree−Fock method with a minimal basis set was used, because it is a good compromise between fast energy and gradient evaluation and acceptable accuracy (vide infra). We utilized the lanl1mb basis set,[19−21] which combines a minimal basis with relativistic effective core potentials for rhodium, phosphorus, and chlorine. Then an inner layer consisting of the most important part of the molecule is calculated both at a high level of theory (E_{inner}^{high}) and the low level previously used for the entire complex (E_{inner}^{low}). The energy difference between these two calculations for the inner layer is then added as an extrapolation to the low-level energy from the first step to get an estimated electronic energy for the complete molecule at the high level of theory as shown in eq 1. As the high-level method, we used a B3LYP density

$$E_{tot}^{high} \approx E_{tot}^{low} + (E_{inner}^{high} - E_{inner}^{low}) \qquad (1)$$

functional calculation[22] with the lanl2dz[19−21] basis set. In this

paper, this combination of two methods will be abbreviated as "ONIOM(B3LYP/lanl2dz:HF/lanl1mb)".

For all calculations, we selected the complete "generic" complex with all organic substituents replaced by hydrogen atoms as the inner layer system, modeling only the substituent effects by ONIOM. These auxiliary hydrogen atoms ("link atoms") are positioned collinear to the P−C bond of the carbon atom they replace. The P−H distance is determined to be a given fraction of the P−C bond length, which enters the calculation as a parameter *f*. See Figure 1 for a pictorial representation of our inner layer system. For the parameter *f*, the default value of the ONIOM implementation[23] in the Gaussian 98 set of programs[24] (i.e., for P−C bonds *f* = 0.773 169) has been used. The suitability of this approach for the actual problem has been tested by calculations on the system with R = methyl, for which both complete DFT and ONIOM calculations can be applied.

All molecular structures were completely optimized either at the B3LYP/lanl2dz or at the ONIOM(B3LYP/lanl2dz:HF/ lanl1mb) levels using analytically calculated gradients. Whenever possible, symmetry constraints have been exploited. All stationary points were characterized by inspection of the eigenvalues of the analytically calculated Hessian matrices, and in nontrivial cases, the topology of the energy hypersurface was determined by evaluation of the intrinsic reaction coordinate[25] (at the B3LYP/lanl2dz level for R = methyl). Estimates for ΔG were calculated within the rigid rotor/harmonic oscillator approximation. For this we relied on the assumption that errors in the ONIOM calculations introduced by the poor quality of the harmonic frequencies for the outer layer will have the same sign and therefore cancel. Scalar relativistic corrections to the electronic energy are included implicitly in our calculations by the use of the relativistic effective core potentials of Hay and Wadt[19−21]—at both the "high" and "low" levels—for the elements rhodium, phosphorus, and chlorine. In addition, single-point energy calculations at the B3LYP/lanl2dz+p or the ONIOM(B3LYP/lanl2dz+p:B3LYP/lanl2dz) level have been

(17) Cao, Z.; Hall, M. B., preprint, communicated to the authors.
(18) Svensson, M.; Humbel, S.; Froese, R. D. J.; Matsubara, T.; Sieber, S.; Morokuma, K. *J. Phys. Chem.* **1996**, *100*, 19357−19363.
(19) Hay, P. J.; Wadt, W. R. *J. Chem. Phys.* **1985**, *82*, 270−283.
(20) Wadt, W. R.; Hay, P. J. *J. Chem. Phys.* **1985**, *82*, 284−298.
(21) Hay, P. J.; Wadt, W. R. *J. Chem. Phys.* **1985**, *82*, 299−310.

(22) Becke, A. D. *J. Chem. Phys.* **1993**, *98*, 5648−5653.
(23) Dapprich, S.; Komáromi, I.; Byun, K. S.; Morokuma, K.; Frisch, M. J. *J. Mol. Struct.: THEOCHEM* **1999**, *461−462*, 1−21.
(24) Frisch, M. J.; Trucks, G. W.; Schlegel, H. B.; Scuseria, G. E.; Robb, M. A.; Cheeseman, J. R.; Zakrzewski, V. G.; Montgomery, J. A., Jr.; Stratmann, R. E.; Burant, J. C.; Dapprich, S.; Millam, J. M.; Daniels, A. D.; Kudin, K. N.; Strain, M. C.; Farkas, O.; Tomasi, J.; Barone, V.; Cossi, M.; Cammi, R.; Mennucci, B.; Pomelli, C.; Adamo, C.; Clifford, S.; Ochterski, J.; Petersson, G. A.; Ayala, P. Y.; Cui, Q.; Morokuma, K.; Malick, D. K.; Rabuck, A. D.; Raghavachari, K.; Foresman, J. B.; Cioslowski, J.; Ortiz, J. V.; Stefanov, B. B.; Liu, G.; Liashenko, A.; Piskorz, P.; Komaromi, I.; Gomperts, R.; Martin, R. L.; Fox, D. J.; Keith, T.; Al-Laham, M. A.; Peng, C. Y.; Nanayakkara, A.; Gonzalez, C.; Challacombe, M.; Gill, P. M. W.; Johnson, B.; Chen, W.; Wong, M. W.; Andres, J. L.; Gonzalez, C.; Head-Gordon, M.; Replogle, E. S.; Pople, J. A. *Gaussian 98*, Revision A.7/, Gaussian, Inc., Pittsburgh, PA, 1998.
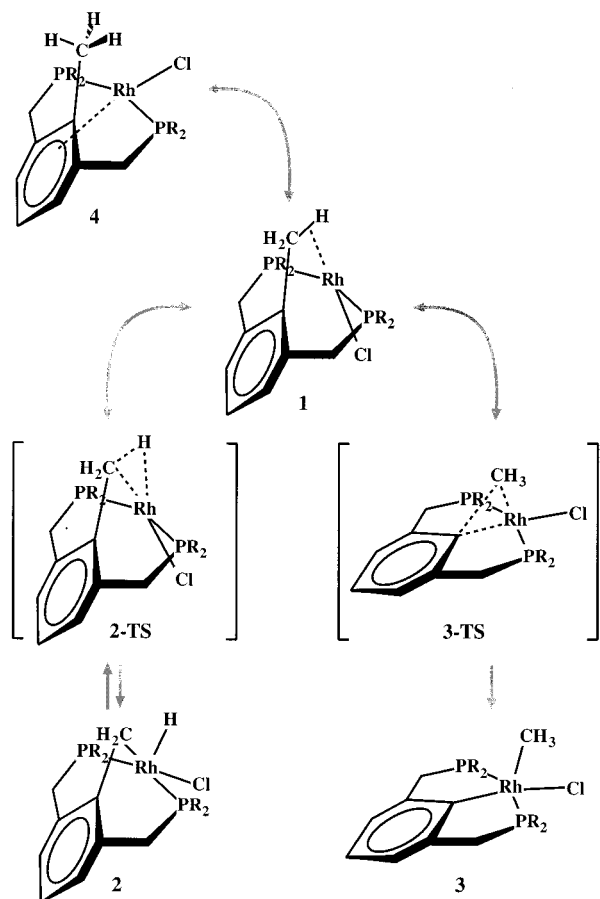(25) Gonzales, C.; Schlegel, H. B. *J. Phys. Chem.* **1990**, *94*, 5523.

Figure 2. Schematic representation of the stationary points involved in the CH/CC activation starting from one common intermediate structure.

performed to get more reliable thermochemical data. The basis set lanl2dz+p consists of the lanl2dz basis set augmented by a single *f* function on Rh[26,27] and the standard D95V(d) basis set[28] on first- and second-row atoms. For all calculations, the Gaussian 98 set of programs[24] was used, running on the SGI Origin 2000 of the Faculty of Chemistry of the Weizmann Institute and on SGI Octane and Compaq XP 1000 workstations in our laboratory.

Atomic partial charges were computed using the natural population analysis (NPA) method[29] as implemented in Gaussian 98; bond orders, in this analysis, are calculated according to Wiberg.[30]

Results and Discussion

1. Optimized Structures. For a reaction pathway involving the CH and CC products, we found six relevant stationary points on the energy hypersurface (Figure 2).

The C−H agostic intermediate structure **1** (Table 1), the product of the CH insertion **2** (Table 3), and the product of the CC insertion **3** (Table 4) are linked by the two corresponding

(26) Höllwarth, A.; Böhme, M.; Dapprich, S.; Ehlers, A. W.; Gobbi, A.; Jonas, V.; Köhler, K. F.; Stegmann, R.; Veldkamp, A.; Frenking, G. *Chem. Phys. Lett.* **1993**, *208*, 237−240.
(27) Ehlers, A. W.; Böhme, M.; Dapprich, S.; Gobbi, A.; Höllwarth, A.; Jonas, V.; Köhler, K. F.; Stegmann, R.; Veldkamp, A.; Frenking, G. *Chem. Phys. Lett.* **1993**, *208*, 111−114.
(28) Dunning, T. H., Jr.; Hay, P. J. In *Modern Theoretical Chemistry*; Schaefer, H. F., III., Ed.; Plenum: New York, 1976.
(29) Reed, A. E.; Curtiss, L. A.; Weinhold, F. *Chem. Rev.* **1988**, *88*, 899−926.
(30) Wiberg, K. B. *Tetrahedron* **1968**, *24*, 1083−1096.

transition states for the CH activation **TS-2** (Table 3) and for the CC activation process **TS-3** (Table 4). Only in the case of R = phenyl another local minimum **4** becomes important because for this system a stationary point with structure **1** is absent. For all other systems, **4** is a local minimum which is not directly related to the interconversion reaction of the CH product to the CC product. The qualitative three-dimensional appearance of structures **1**−**3** is shown in Figure 3 for the simplest example, the complex with hydrogen substituents at the phosphorus atoms (the ligand cores of the other complexes have similar structures). A perspective representation of structure **4** is given in Figure 4 for the complex with R = phenyl.

Along the entire reaction pathway, both chelating phosphorus atoms remain bound to the transition metal atom. If not explicitly noted, all stationary points adopt C_s symmetry. The mirror plane bisects the molecule perpendicular to the plane of the phenyl ring; the phosphorus atoms are symmetry equivalent. This was found for most of the compounds included in this study. Concerning this point, it has to be noted as a warning that a proper choice of the grid used for numerical integrations to solve the Kohn−Sham and coupled perturbed Kohn−Sham (CPKS) equations is imperative: if this grid is too coarse, artifactual symmetry breaking occurs.[31] For example, structure **3** with R = methyl (C_s symmetry) appears as a transition state at the B3LYP/lanl2dz level, when the default grids of Gaussian 98 (i.e., (75 302)-pruned[32] for the integration and (35 110)-pruned for the CPKS equations) are used. Only with finer integration grids ((99 590)-pruned and (75, 302)-pruned, respectively) is the proper curvature of the energy hypersurface obtained.

1.1. The Intermediate Structure. According to ligand field arguments, for the rhodium(I) complex **1** (i.e., d[8] low-spin configuration), a square planar ligand field is most stable, while for the product complexes **2** and **3** (rhodium(III), i.e., d[6] low-spin configuration) a square pyramidal or octahedral (if an additional ligand is present) arrangement of ligands will result in stable ligand fields. For this local arrangement of ligands an angle ∠P−Rh−P of ∼180° should be optimal, which is consistent with the optimized structure for the T-shaped complex fragment RhCl(PH$_3$)$_2$. Here a value for ∠P−Rh−P of 172.9° is found at the B3LYP/lanl2dz level. (A detailed analysis of CH bond activation by the RhCl(PH$_3$)$_2$ fragment was given by Koga and Morokuma.[12,33]) Transferring this to the chelating PCP ligand, one can expect that an interaction of the transition metal center and the bonds to be cleaved can be achieved without introducing much strain. In addition to an optimal P−M−P angle, another source of strain (i.e., nonoptimal local arrangement of atoms) can become important in the intramolecular bond activation reaction: the free coordination site of the T-shaped complex fragment for interactions with the bonds to be cleaved is in trans position of the chloro ligand. This implies that the formation of, for example, a weak agostic interaction is very sensitive to steric effects altering the position of the chloro ligand.

For all compounds included in our study (with one exception), the intermediate structure on the reaction pathway corresponds to **1**. It is best described as a weak complex of a 3-fold coordinated transition metal ion and the C−H bond of the methyl group as a fourth "ligand". Examples for agostic

(31) Martin, J. M. L.; Bauschlicher, C. W.; Ricca, A. *Comput. Phys. Commun.*, in press.
(32) For more information about these grids, see: the Gaussian 98 Users Manual or its on-line version (URL: http://www.gaussian.com/techin-fo.htm).
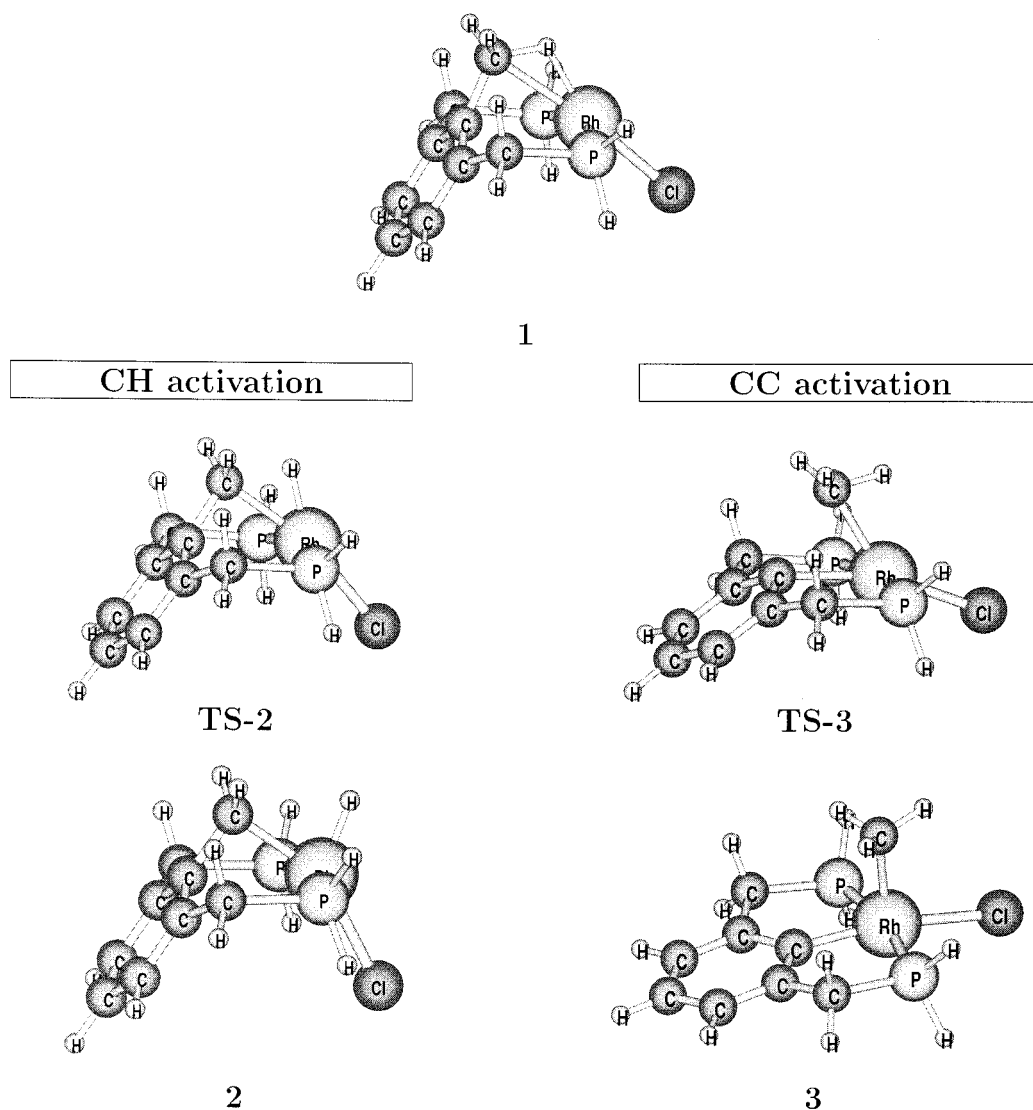(33) Koga, N.; Morokuma, K. *J. Phys. Chem.* **1990**, *94*, 5454−5462.

Figure 3. Perspective view of all stationary points shown in Figure *x*. All structures are optimized at B3LYP/lanl2dz level and visualized using Molden.[48]

interactions involving rhodium complexes and C−H bonds are known,[34,35] and similar complexes of transition metal atoms and C−H σ bonds have been described previously in the literature as entry channels for reactions of naked transition metal atoms[10,36−38] or transition metal complexes[9,11,12,33,35,39−43] with methane.

Due to the agostic interaction, which is caused by charge donation from the C−H σ bond to the rhodium atom accompanied by back-donation into the antibonding σ^* orbital, the C−H bond is weakened. This can be witnessed in a pronounced red shift of the corresponding harmonic stretching

mode relative to that of the noninteracting C−H bonds of the methyl group, which are close to the value calculated for the uncoordinated ligand (see Table 2). The agostic interaction can also be observed from the NPA charges (at the B3LYP/lanl2dz level for the case of R = H): A bond order of 0.78 is found for the interacting C−H bond while the two other C−H bonds of the methyl group have bond indices of 0.91.

The situation is different only for R = phenyl. The complex with an agostic interaction is found to be no stationary point on the energy hypersurface. Therefore, structure **4**, which is a local minimum for complexes with other substituents, too, becomes important for the reaction pathway. This structure (for parameters, see Table 1) is best described as an interaction between the rhodium atom and the π system of the phenyl ring. A perspective view of this structure is given in Figure 4 for R = phenyl.

Because in the case R = Cl a minimum corresponding to the agostic interaction is found, the different behavior in the case R = phenyl has to be assigned to steric rather than electronic effects of the phenyl substituents: The rhodium-bound chloride ligand is forced into a position strongly disfavoring an agostic interaction with the free coordination site in its trans position. As the reader may verify by inspection of Figure 4, a very small angle ∠H−Rh−C would result in this case. The reaction

(34) Vigalok, A.; Uzan, O.; Shimon, L. J. W.; Ben-David, Y.; Martin, J. M. L.; Milstein, D. *J. Am. Chem. Soc.* **1998**, *120*, 12539−12544.

(35) Hall, C.; Perutz, R. N. *Chem. Rev.* **1996**, *96*, 3125−3146.

(36) Siegbahn, P. E. M.; Blomberg, M. R. A. *J. Am. Chem. Soc.* **1992**, *114*, 10548−10556.

(37) Westerberg, J.; Blomberg, M. R. A. *J. Phys. Chem. A* **1998**, *102*, 7303−7307.

(38) Sändig, N.; Koch, W. *Organometallics* **1997**, *16*, 5244−5251.

(39) Saillard, J.-L.; Hoffmann, R. *J. Am. Chem. Soc.* **1984**, *106*, 2006−2026.

(40) Ziegler, T.; Tschinke, V.; Fan, L.; Becke, A. D. *J. Am. Chem. Soc.* **1989**, *111*, 9177−9185.

(41) Song, J.; Hall, M. B. *Organometallics* **1993**, *12*, 3118−3126.

(42) Heiberg, H.; Swang, O.; Ryan, O. B.; Gropen, O. *J. Phys. Chem. A* **1999**, *103*, 10004−10008.

(43) Siegbahn, P. E. M. *J. Am. Chem. Soc.* **1996**, *118*, 1487−1496.

Table 1. Structural Parameters for Structures **1** and **4** (Bond Lengths in Å; Angles in deg)

				Structure **1**				
R	RhC$_{Ph}$	RhC	RhH	RhP	RhCl	PRhP	CRhCl	HRhC
tert-butyl[a]	2.561	2.549	1.920	2.415	2.440	161.4	165.4	24.9
isopropyl	2.604	2.488	1.842	2.385	2.421	159.0	176.5	26.0
methyl[a]	2.639	2.486	1.825	2.372	2.413	155.0	178.2	26.1
methyl[b]	2.604	2.459	1.813	2.402	2.408	158.1	175.6	26.8
H[b]	2.668	2.488	1.816	2.395	2.388	154.6	173.7	26.0
Cl[b]	2.838	2.610	1.867	2.374	2.335	145.5	174.0	23.0

			Structure **4**			
R	RhC$_{ipso}$	RhC$_{ortho}$	RhC$_{meth}$	RhP	RhCl	PRhP	C$_{ipso}$RhCl
tert-butyl[a]	2.441	2.908	3.083	2.403	2.452	171.7	171.0
isopropyl[a]	2.389	2.885	3.066	2.381	2.440	171.9	163.6
methyl[a]	2.377	2.859	3.059	2.355	2.426	170.8	160.0
methyl[b]	2.368	2.856	3.044	2.382	2.423	171.5	158.1
H[b]	2.404	2.880	3.056	2.382	2.402	170.1	160.4
phenyl[a]	2.396	2.863	3.063	2.386	2.446	169.9	169.2
Cl[b]	2.515	2.947	3.151	2.363	2.344	161.7	162.9

[a] ONIOM(B3LYP/lanl2dz:HF/lanl1mb).   [b] B3LYP/lanl2dz.

Table 2. Vibrational Frequencies for the C−H Stretching Modes in the Weakly Bound Methyl Group in the Intermediate Structure (in cm^{-1}, Calculated in the Harmonic Approximation, Unscaled)

R	CH(bound)	CH(unbound)	free ligand
tert-butyl[a]	2496	3108, 3172	3027, 3108, 3184
isopropyl[a]	2314	3103, 3167	3027, 3112, 3180
methyl[b]	2214	3095, 3157	3028, 3118, 3168
H[b]	2243	3096, 3158	3030, 3126, 3162
phenyl[a]		3007, 3131, 3172	3027, 3124, 3160
Cl[b]	2450	3106, 3169	3039, 3105, 3163

[a] ONIOM(B3LYP/lanl2dz:HF/lanl1mb).   [b] B3LYP/lanl2dz.

Figure 4. Schematic representation and perspective view of complex **4** with phenyl substituents.

Table 3. Structural Parameters for the CH Insertion Product and the Corresponding Transition State (Bond Lengths in Å; Angles in deg)

R	RhH	RhC	RhP	RhCl	PRhP	CRhCl	HRhC	RhCC$_{Ph}$
				Product **2**				
tert-butyl[a]	1.522	2.126	2.446	2.524	159.6	184.6[c]	86.5	91.8
isopropyl[a]	1.528	2.129	2.397	2.505	162.7	175.8	89.5	89.3
methyl[a]	1.534	2.136	2.376	2.490	164.0	168.8	89.2	87.5
methyl[b]	1.531	2.122	2.408	2.489	162.6	167.1	85.6	89.6
H[b]	1.539	2.121	2.400	2.471	159.1	151.6	76.7	92.5
phenyl[a]	1.525	2.136	2.402	2.481	163.2	173.2	87.1	88.7
Cl[b]	1.544	2.152	2.380	2.418	156.2	145.6	73.5	92.5
			Transition State **TS-2**					
tert-butyl[a]	1.585	2.259	2.437	2.461	157.6	184.9[c]	41.4	
tert-butyl[b]	1.583	2.250	2.459	2.465	157.7	183.5[c]	41.6	
isopropyl[a]	1.596	2.248	2.397	2.445	157.5	175.5	40.7	
methyl[a]	1.606	2.251	2.383	2.435	156.3	170.9	40.2	
methyl[b]	1.606	2.243	2.413	2.430	157.4	169.5	40.3	
H[b]	1.607	2.242	2.400	2.414	155.7	165.3	40.7	
phenyl[a]	1.596	2.254	2.397	2.427	158.9	175.3	41.1	
Cl[b]	1.594	2.254	2.386	2.370	152.4	164.1	43.7	

[a] ONIOM(B3LYP/lanl2dz:HF/lanl1mb).   [b] B3LYP/lanl2dz.   [c] Angles of >180° occur because the angle opposite to the hydrogen atom is given.

In the hydride complex **2**, the rhodium atom is coordinated square pyramidally. The hydrogen atom occupies the apical position and the chloro ligand is coordinated trans to the rhodium carbon bond. The small valence angle of ∼90° at the coordinated methylene carbon (∠Rh−C−C) indicates the occurrence of some strain in this molecule. In other words, the benzylic rhodium carbon bond in the CH product is rather weak because the rigidity of the chelate core inhibits an optimal overlap (i.e., a valence angle of ∼109°). NPA (at the B3LYP/lanl2dz level for R = H) shows a C−Rh bond order of only 0.53 whereas for the CC product a bond order of 0.80 for the C$_{sp^3}$−Rh bond is found.

A comparison of complexes with different phosphine substituent "R" reveals a dependence of the angle ∠C−Rh−Cl on the sterical demand of the substituent. The angle increases in the series Cl < H < methyl < isopropyl ≈ phenyl < *tert*-butyl. This point will be discussed in more detail below.

1.3. C−C Insertion. The insertion of the rhodium atom into the C−C bond is accompanied by large-amplitude nuclear motions of the complete ligand system. In the course of the reaction from **1** to **3**, both rhodium carbon distances are reduced by ∼0.5 Å. The resulting methyl complex shows an almost

coordinates from **4** to the transition states **TS-2** and **TS-3** involve the rotation of the methyl group by 30°. The transition state for the methyl rotation is found to be only 3.1 kJ·mol^{-1} above **4** (R = phenyl at the ONIOM(B3LYP/lanl2dz:HF/lanl1mb) level).

1.2. C−H Insertion. Upon insertion of the rhodium atom into the C−H bond, only minor changes occur in the nuclear coordinates of the chelating ligand. The reaction coordinate is dominated by the change in the H−Rh−C angle, which is widened from ∼25° in **1** to ∼90° in **2**. The three-centered transition state is found quite early on this reaction coordinate (∠H−Rh−C ∼41°). This reaction coordinate is very similar to that found by Koga and Morokuma[12,33] for the reaction of RhCl-(PH$_3$)$_2$ with methane.

Table 4. Structural Parameters for the CC Insertion Product (Bond Lengths in Å; Angles in deg)

R	RhC$_{Ph}$	RhC	RhP	RhCl	PRhP	CRhCl	CRhC$_{Ph}$
			Product **3**				
tert-butyl[a]	2.045	2.060	2.414	2.531	162.8	175.0	82.2
tert-butyl[b]	2.050	2.055	2.359	2.489	162.6	175.3	81.0
tert-butyl[c]	*2.02(2)*	*2.17(2)*	*2.333(5)*	*2.470(4)*	*164.6(2)*	*179.1(5)*	*80.3(8)*
isopropyl	2.037	2.071	2.379	2.527	165.5	155.9	81.8
methyl[a]	2.037	2.071	2.379	2.527	165.5	155.9	81.8
methyl[d]	2.039	2.067	2.367	2.513	167.6	161.9	86.1
H[d]	2.057	2.072	2.360	2.488	167.5	169.6	91.5
phenyl[a]	2.052	2.064	2.356	2.529	164.3	171.1	87.8
Cl[d]	2.105	2.084	2.325	2.431	161.7	170.9	91.1
			Transition State **TS-3**				
tert-butyl[a]	2.117	2.274	2.409	2.474	162.8	166.8	49.4
tert-butyl[b]	2.116	2.277	2.428	2.475	164.0	167.3	49.4
isopropyl[a]	2.104	2.273	2.373	2.462	165.5	152.3	49.7
methyl[a]	2.113	2.266	2.352	2.455	162.7	151.0	49.8
methyl[d]	2.111	2.274	2.380	2.448	164.4	149.5	49.7
H[d]	2.127	2.276	2.371	2.428	162.1	155.4	49.5
phenyl[a]	2.110	2.262	2.378	2.470	165.5	161.1	50.3
Cl[d]	2.144	2.281	2.344	2.380	160.3	152.9	51.4

[a] ONIOM(B3LYP/lanl2dz:HF/lanl1mb). [b] ONIOM(B3LYP/lanl2dz+p:HF/lanl1mb). [c] Exp.[7] [d] B3LYP/lanl2dz.

planar structure of the basal chelate core of the squared pyramidal complex (in contrast to structures **1** and **2**). Again, the 5-fold coordinated rhodium atom has a square pyramidal ligand field with the methyl group in the apical position. It has to be noted that the square pyramidal conformation of the C−C insertion product is much less distorted than in the C−H insertion product.

A comparison of the calculated and experimental[7] structures with R = *tert*-butyl shows them to be in good agreement. The largest deviation is observed for the Rh−C bond of the methyl group ($\Delta r = 0.12$ Å). Because all other structural parameters are in far better agreement, it might be assumed that an intermolecular interaction due to crystal packing is responsible for the longer bond found in the experiment.

1.4. Binding of Additional Ligands. The pentacoordinated insertion product complexes (**2** and **3**) have one free coordination site to which another ligand can bind. In the experiment this could be either a solvent molecule[44] or for example phosphines added to the reaction mixture.[16] PH$_3$ was used as a model compound for the calculations.

Products (d^6 Complexes). Following simple ligand field arguments leads to the assumption that for the product complexes **2** and **3** only minor structural changes will occur upon binding of an additional ligand "L". Taking all permutations into account, several isomers are possible.

We considered the structures **2-L$_{ax}$** (**3-L$_{ax}$**, respectively) and **2-L$_{eq}$** (**3-L$_{eq}$**) (see Figure 5). Our computational results are in agreement with experimentally determined structures, which are available for **2-L$_{eq}$**, R = phenyl[5,16] and **3-L$_{eq}$**, R = methyl[16] (see Table 5).

A comparison of bond lengths reveals that all rhodium−ligand bonds become longer if an additional ligand is introduced. The largest effect is observed for the ligand that was in the apical position of the tetragonal pyramid prior to coordination (i.e., the hydrogen atom in **2** or the methyl group in **3**).

A qualitative inspection of the calculated structures **2-L$_{ax}$** and **2-L$_{eq}$** suggests that the additional ligand cannot bind optimally to the rhodium atom. Due to the bent structure of the chelate core of the complex, a ligand in axial position engages in a repulsive interaction with the phenyl ring. This is also reflected in the structural parameters: The axial ligand is a very long

(44) Rybtchinski, B.; Milstein, D. *J. Am. Chem. Soc.* **1999**, *121*, 4528−4529.

distance from the rhodium atom and the angle ∠Rh−C−C is widened by more than 10° relative to **2**.

In the case of the CC product, the most obvious effect of the phosphine ligand on the structure is the loss of C_s symmetry. The phenyl ring is twisted out of the equatorial plane of the rhodium coordination octahedron. Consequently, the two chelating phosphorus atoms are no longer equivalent. Again, the reason for this distortion is steric crowding at the axial coordination sites. By the observed conformational change, the repulsive interaction between the substituents at the phosphorus atoms and the axial ligands of the rhodium atom is minimized. The reader may verify this by comparing the orientation of the substituents in Figure 5 with that in Figure 8 (left).

Transition States. In addition to the product complexes, we also examined the influence of a phosphine ligand binding to the transition states of the CH and CC activation for R = methyl and phenyl. We restricted our calculations to complexes with the PH$_3$ ligand in trans position to the H or CH$_3$ group, respectively. Some optimized structural parameters are given in Table 6.

Interestingly, the phosphine ligand remains in trans position to the hydrogen atom or the methyl group. Valence angles larger than 170° are found. Thus, the reaction from the CH product **2-L$_{ax}$** (or the CC product **3-L$_{ax}$**, respectively) to the corresponding transition state **TS-2-L** may be described as a rotation of the H−Rh−PH$_3$ axis relative to the equatorial plane (formed by the remaining four ligands). In the product complexes, it adopts a perpendicular orientation, whereas in the transition state, the angle H−Rh−C (or C−Rh−C for the CC cleavage) becomes much smaller than 90° (∼50°). As a consequence, the Cl−Rh−P′ angle also becomes smaller and due to the increased P−Cl interaction the Rh−Cl bond is stretched. Qualitatively the transition-state structure can be described as a strongly distorted octahedral complex (formally assigning a d^6 configuration to the transition metal atom). In the case of structure **TS-2-L** with R = methyl, no hexacoordinate stationary point could be located. A relaxed surface scan (i.e., varying the value of one parameter (e.g., bond length or angle) in a controlled manner while optimizing all others) revealed that the potential energy hypersurface in the region of the transition state is very flat and dissociative with respect to Rh−P′ bond stretch. This result is plausible since already in structure **2-L$_{ax}$** a very long Rh−P′ bond was found.
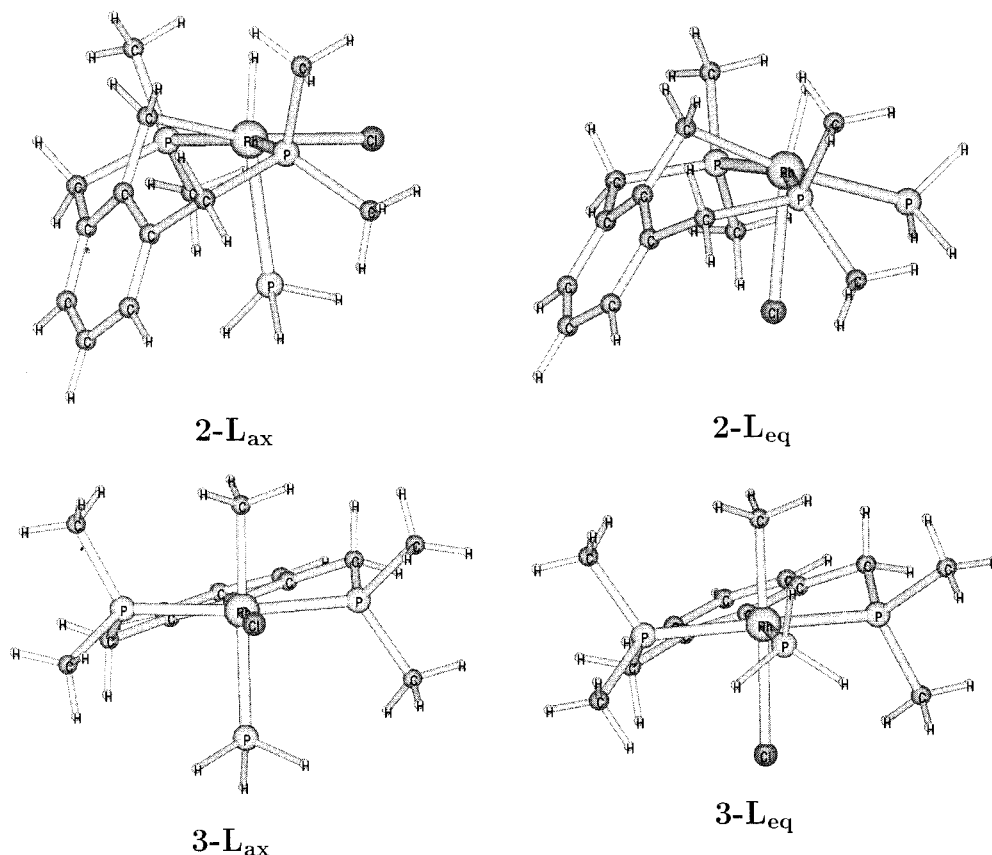
Figure 5. Perspective view of complexes with an additional phosphine ligand (the complexes with R = phenyl have similar structures for the chelate core)

Table 5. Structural Parameters for CH Product and CC Product Complexes with an Additional Phosphine Ligand (Bond Lengths in Å; Angles in deg)

R	RhH	RhC	RhP	RhCl	RhP′	PRhP	CRhCl	CRhH	P′RhC	RhCC$_{Ph}$
					CH Products					
					PH$_3$ Axial					
methyl[a]	1.545	2.158	2.379	2.546	2.712	156.4	191.5[d]	80.7	111.5	97.3
phenyl[a]	1.540	2.154	2.423	2.573	2.655	156.0	197.1[d]	78.2	112.9	97.5
					PH$_3$ Equatorial					
methyl[a]	1.564	2.153	2.392	2.642	2.487	152.8	105.5	80.4	188.0[d]	100.3
phenyl[a]	1.554	2.151	2.414	2.625	2.481	153.2	107.9	81.3	186.0[d]	100.5
phenyl[b,c]		*2.142*	*2.335*		*2.371*	*145.5*			*184.2*[d]	*103.6*

R	RhC$_{Ph}$	RhC	RhP	RhCl	RhP′	PRhP	C$_{Ph}$RhCl	CRhC$_{Ph}$	P′RhC$_{Ph}$
					CC Products				
					PH$_3$ Axial				
methyl[a]	2.063	2.108	2.359, 2.361	2.570	2.552	164.4	178.6	91.1	98.9
phenyl[a]	2.062	2.106	2.377, 2.392	2.592	2.550	164.5	177.5	90.6	97.3
					PH$_3$ Equatorial				
methyl[a]	2.074	2.114	2.360, 2.366	2.600	2.515	162.5	95.1	90.3	176.4
methyl[b]	*2.094*	*2.114*	*2.287*		*2.372*	*157.6*		*88.4*	*178.2*
phenyl[a]	2.070	2.114	2.380, 2.408	2.598	2.529	162.7	93.3	90.2	173.4

[a] ONIOM(B3LYP/lanl2dz:HF/lanl1mb). [b] Experimental structure,[16] [c] This isomer differs from the calculated molecule in interchanged H and Cl positions. [d] See Table 3.

Intermediate Structures. In the intermediate structure, the rhodium atom has a d^8 configuration. This favors a square planar arrangement of ligands. If an additional PH$_3$ molecule binds to the rhodium atom, it substitutes the weakest bound ligand, in this case the weak agostic bond. According to our calculations, a structure corresponding to **1** or **4** with an additional phosphine ligand exhibits no interaction between the rhodium atom and the methyl group of the PCP ligand. Qualitatively, the structure of **1-L** is shown in Figure 6.

The complex shows a square planar arrangement of ligands, and the plane formed by the coordinating atoms is approximately parallel to the plane of the phenyl ring. (For selected structural parameters see Table 7) The deviations from planarity of both the ligand field of the rhodium atom and the phenyl ring can be explained by the occurrence of strain due to (a) the nonoptimal position of the phosphine "arms" of the PCP ligand and (b) the close proximity of one of the remaining ligands to the phenyl ring. We considered only one isomer (with the

Table 6. Structural Parameters for the Transition States of CC and CH Activation with an Additional Phosphine Ligand (Calculated at ONIOM(B3LYP/lanl2dz:HF/lanl1mb) Level) (Bond Lengths in Å; Angles in deg).

R	RhX[a]	RhC	RhP	RhCl	RhP′	PRhP	CRhCl	CRhX[a]	P′RhCl	P′RhX
				CH Activation						
methyl					b					
phenyl	1.624	2.302	2.400	2.730	2.478	157.2	134.1	38.0	75.9	171.9
				CC Activation						
methyl	2.338	2.135	2.360	2.710	2.421	168.3	155.9	47.5	81.3	170.3
phenyl	2.314	2.141	2.396	2.822	2.450	167.4	160.0	47.9	73.5	174.4

[a] X = H for CH activation and CH_3 for CC activation. [b] No stationary point could be found for this TS: PH_3 is unbound.
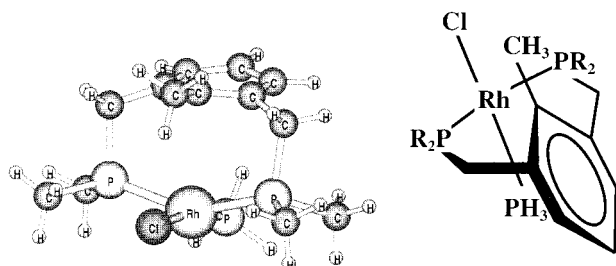
Figure 6. Perspective view of the structure **1-L** (R = methyl; the structures for R = phenyl are similar).

Table 7. Selected Structural Parameters for Complex **1-L** Calculated at ONIOM(B3LYP/ lanl2dz:HF/lanl1mb) Level (Bond Lengths in Å; Angles in deg)

	R = Me	R = Ph
RhP	2.392	2.418
RhP′	2.348	2.352
RhCl	2.463	2.459
PRhP	149.8	151.7
P′RhCl	166.1	168.4

Table 8. Relative Energies (Relative to 1) of the Stationary Points on the Energy Hypersurface (in kJ·mol^{-1})

		CH insertion		CC insertion	
R	4	TS-2	2	TS-3	3
tert-butyl[a]	−3.8	23.2	−29.5	45.9	−47.3
tert-butyl[c]	−4.9	20.1	−24.8	45.1	−45.5
tert-butyl[d]	−9.1	24.3	−14.7	42.6	−40.4
isopropyl[a]	−2.3	16.1	−37.1	43.5	−45.5
isopropyl[c]	−3.6	14.2	−31.2	42.4	−44.6
isopropyl[d]	−9.0	17.2	−23.3	40.4	−38.5
methyl[a]	−3.1	14.6	−38.3	48.3	−48.0
methyl[b]	−1.7	12.8	−32.3	48.0	−47.1
methyl[c]	−2.0	13.0	−31.4	47.9	−47.4
methyl[d]	−8.6	16.0	−23.9	46.5	−40.2
methyl[e]	−3.9	15.2	−25.5	45.8	−41.9
H[b]	−1.8	14.6	−24.4	55.2	−35.2
H[e]	−8.0	16.8	−16.5	53.5	−28.1
phenyl[a]	f	42.2	−3.2	62.4	−35.7
phenyl[c]	f	42.2	−2.2	65.3	−35.6
phenyl[d]	f	50.5	15.4	69.9	−25.8
Cl[b]	−1.4	32.2	7.2	79.0	6.6
Cl[e]	−9.8	29.2	2.3	65.3	−15.9

[a] ONIOM(B3LYP/lanl2dz:HF/lanl1mb). [b] B3LYP/lanl2dz. [c] B3LYP/ lanl2dz//ONIOM(B3LYP/lanl2dz:HF/lanl1mb). [d] ONIOM(B3LYP/ lanl2dz+p:B3LYP/lanl2dz)//ONIOM(B3LYP/lanl2dz:HF/lanl1mb). [e] B3LYP/lanl2dz+p//B3LYP/lanl2dz. [f] Energies relative to **4**.

Table 9. Changes in the Gibbs Free Energy (ΔG (298 K)) and the Enthalpy (ΔH (298 K), in Parentheses) Relative to **1** (in kJ·mol^{-1}) Including (Unscaled) Zero-Point Vibrational Energies and Thermal Corrections.

		CH insertion		CC insertion	
R	4	TS-2	2	TS-3	3
tert-butyl[a]	−9.8 (−2.4)	19.3 (13.7)	−30.2 (−35.1)	43.1 (40.1)	−56.0 (−49.8)
isopropyl[a]	−6.0 (0.8)	12.7 (7.6)	−37.2 (−42.2)	50.2 (52.5)	−54.4 (−47.0)
methyl[b]	−9.8 (−0.3)	6.2 (3.6)	−40.3 (−38.7)	42.1 (42.3)	−62.0 (−49.9)
H[b]	−6.4 (0.3)	7.9 (5.0)	−28.5 (−29.7)	50.8 (49.9)	−48.6 (−40.0)
phenyl[a]		29.8 (29.3)	−19.6 (−12.5)	57.4 (54.0)	−53.2 (−41.4)
Cl[b]	−6.5 (1.0)	27.8 (22.7)	4.4 (1.4)	74.8 (72.9)	−1.3 (3.2)

[a] ONIOM(B3LYP/lanl2dz:HF/lanl1mb). [b] B3LYP/lanl2dz.

phosphine ligand close to the phenyl ring) because our calculations give evidence that the ligand in this position dissociates in the course of the activation reactions (it is very weakly bound in the transition state) and we are interested in the neutral complexes in which the chloro ligand remains bound.

2. Energetic Considerations. Our calculated energies relative to structure **1** are listed in Table 8 (see also Figure 7); values for ΔG^{298K} are given in Table 9. As a qualitative result, independent of the identity of the ligand and the level of theory employed, our calculations demonstrate that the C−H insertion reaction is always kinetically favored, whereas the CC product is the thermodynamically stable one. The intermediate structure **1** is only slightly less stable than **4** (regardless of substituent R: $\Delta E \approx 3.0$ kJ·mol^{-1}). The transition state for the conversion of **1** to **4** is quite low. We calculated an energy difference of 10.1 kJ·mol^{-1} relative to **1** for R = methyl. Thus, the methyl group can "slide" easily along the rhodium atom allowing a facile CC and CH bond cleavage.

2.1. Comparison with Experimental Data. On the basis of kinetic measurements for R = *tert*-butyl,[7] the CC and CH activation reactions are found to have essentially equal barrier heights. The discrepancy of ∼20 kJ·mol^{-1} in $\Delta\Delta G^{\ddagger}$ between theory and experiment results on one hand from the limitations of the theoretical model (B3LYP density functional with a basis set of valence double-ζ quality) and on the other hand from the fact that in the experiment the measured rates of the actual activation reactions are partially affected by the back reaction of the C−H activation product to **1** (See Scheme 1). Unfortunately, even the present calculations were at the limit of the computational resources available to us and a quantitative calculation of barrier heights within 10 kJ·mol^{-1} is beyond the

scope of the methods applied here.[45] Nevertheless, by test calculations using different exchange-correlation functionals we made sure that no artifactual distortion of the energy hypersurface due to the Hartree−Fock exchange component of the B3LYP functional is responsible for the discrepancies.

2.2. Performance of the ONIOM Model. To test the suitability of the simplifications introduced by our ONIOM model, a series of calculations on the system with R = methyl has been performed since for this system of intermediate size both ONIOM and B3LYP optimizations are feasible. A comparison of the B3LYP/lanl2dz with the ONIOM(B3LYP/lanl2dz: HF/lanl1mb) result shows that the ONIOM calculation is able to reproduce the result of the complete DFT calculation (the

(45) Curtiss, L. A.; Raghavachari, K.; Redfern, P. C.; Pople, J. A. *J. Chem. Phys.* **1997**, *106*, 1063−1078. Baker, J.; Andzelm, J.; Muir, M.; Taylor, P. R. *Chem. Phys. Lett.* **1995**, *237*, 53.
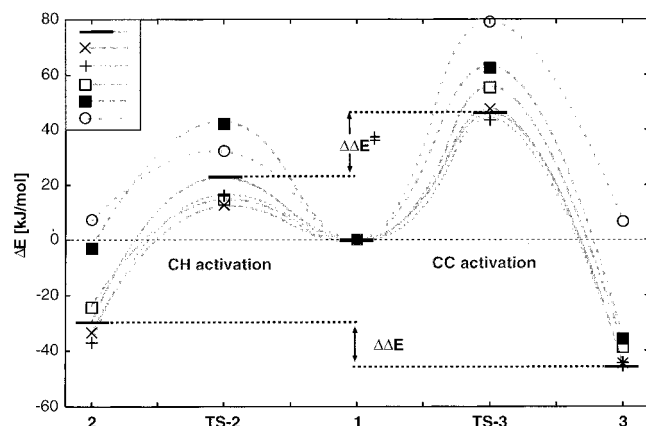
Bond Activation by Rh(I) PCP Pincer Complexes

J. Am. Chem. Soc., Vol. 122, No. 29, 2000 7103

Figure 7. Graphical representation of the reaction coordinates. Key: (−) *tert*-butyl, (×) isopropyl, (+) methyl, (□) H, (■) phenyl, and (○) Cl. For numerical data, see Table 8.
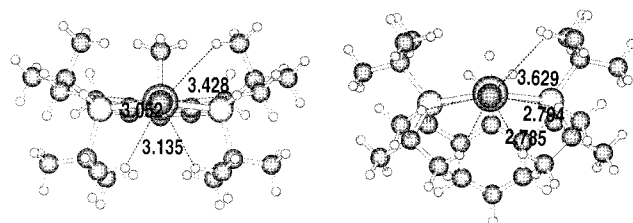

Figure 8. Distances between the chloro ligand and the bulky *tert*-butyl substituents at the phosphorus in the CC (left) and the CH (right) insertion product. The line of sight is along the Cl−Rh bond.

largest energy difference is 6 kJ·mol⁻¹). A B3LYP/lanl2dz single-point calculation with the ONIOM optimized structure reveals that the major part of this error is introduced by the ONIOM energy evaluation. The ONIOM equilibrium structure (at least for the most important inner layer part of the molecule) is in close agreement with the DFT structure. Therefore, the relative energies of these single-point calculations reproduce the DFT optimized results even better. The good performance of the HF/lanl1mb description of the outer layer originates of course from a strong error compensation. Our ONIOM model is applicable as long as steric effects of the substituents in the outer layer dominate. It is expected to fail in cases where electronic effects of the substituents become important.

2.3. Influence of Substituents. The actual height of the activation barriers depends on the substituents at the phosphorus atoms. The computational results show that bulky groups such as the *tert*-butyl group decrease the barrier for CC activation and increase the barrier of CH activation (e.g., R = H, $\Delta\Delta E^{\ddagger}$ = 36.7 kJ·mol⁻¹; R = *tert*-butyl, $\Delta\Delta E^{\ddagger}$ = 18.3 kJ·mol⁻¹; R = phenyl, $\Delta\Delta E^{\ddagger}$ = 19.4 kJ·mol⁻¹). A similar trend can be observed for the relative energies of the products of the two insertion reactions: The relative stability of the methyl complex **3** over the hydride complex **2** is increased if the phosphorus atoms have bulky substituents. (e.g., R = H, $\Delta\Delta E$ = 11.6 kJ·mol⁻¹; R = *tert*-butyl, $\Delta\Delta E$ = 25.7 kJ·mol⁻¹; R = phenyl, $\Delta\Delta E$ = 40.8 kJ·mol⁻¹). The reason for these trends is found in the sterical crowding in the vicinity of the chloro ligand as depicted in Figure 8.

Due to the bent conformation of the complex in the case of the CH insertion product, the chloro ligand is forced closer to the substituents of the phosphorus atoms. This can also be seen in the perspective view given in Figure 2. If the substituents are large, some chlorine−hydrogen distances in the CH insertion product are of the magnitude of the sum of the van der Waals

Table 10. Relative Energies (in kJ·mol⁻¹) for Complexes Containing an Additional Phosphine Ligand

R		1-L	CH insertion			CC insertion		
			TS-2-L	2-L$_{ax}$	2-L$_{eq}$	TS-3-L	3-L$_{ax}$	3-L$_{eq}$
methyl[a]	ΔE_{bind}[d]	−65.4	c	7.1	−25.1	41.2	−35.4	−52.1
methyl[b]		−86.9	c	7.9	−38.1	29.3	−42.3	−62.9
phenyl[a]		−24.3	31.9	−8.0	−26.7	35.2	−37.7	−23.4
phenyl[b]		−42.7	5.2	−19.7	−51.7	9.1	−54.3	−35.1
methyl[a]	ΔE_{rel}[e]	0.0	c	34.2	2.0	154.9	−18.0	−34.6
methyl[b]		0.0	c	71.0	24.9	162.7	4.3	−16.2
phenyl[a]		0.0	99.3	14.0	−4.8	122.8	−48.3	−33.9
phenyl[b]		0.0	102.3	38.4	6.3	117.8	−34.8	−18.2

[a] ONIOM(B3LYP/lanl2dz:HF/lanl1mb). [b] ONIOM(B3LYP/lanl2dz+p: B3LYP/lanl2dz). [c] No stationary point could be located; the hypersurface is dissociative with respect to M−L bond stretch. [d] $\Delta E_{bind} = E(X\text{-}L) - (E(X) + E(L))$. [e] ΔE_{rel} = energies relative to complex **1-L**.

radii (∼2.8 Å). For the CC insertion product, no such contacts can be found.

In addition to these steric effects of the ligand system, our results indicate that electron-withdrawing groups such as phenyl groups or chlorine atoms reduce the ability of the transition metal complex for oxidative addition. It is known from experiment that a complex with phenyl substituents (the chloro compound is hitherto experimentally unknown) shows no C−C activation even at high temperatures.[5,15,16] This finding has been assigned to a strong stabilization of the C−H insertion product relative to the C−C insertion one. The computational results give evidence for a different interpretation: In both cases (R = Ph, Cl), the intermediate structure is almost as stable as the CH insertion product. Therefore, the activation barriers for CH and CC insertion become much higher, and even if the system shows reductive elimination, it gets trapped in the intermediate structure. Instead of C−C bond cleavage, an equilibrium between **2** and **4** has to be expected in this case.

2.4. Influence of Additionally Coordinated Ligands. Energy data for the addition of a phosphine molecule to the product complexes with R = methyl and phenyl are given in Table 10.

Accordingly, the phosphine ligand is always more strongly bound in complexes of the CC product. This is in line with our findings for the molecular structure. In the CH product, the phosphine ligand prefers the equatorial position. The reason for this is a less strained structure when the smaller chloro ligand occupies the axial position. The reader may verify this by comparison of the differences in the metal−ligand distance for equatorial and axial ligands: $\Delta r_{Cl} \approx 0.1$ Å, $\Delta r_P \approx 0.2$ Å. For the CC product, the stabilization depends on the trans influence of the methyl group. Accordingly, the most stable conformation should have the weakest bound ligand in the axial position: This is the chloro ligand. Therefore, the conformer **3-L$_{eq}$** is expected to be most stable. This is only realized for R = methyl. For R = phenyl, the steric demand of the substituents of the phosphorus atoms predominates, which favors **3-L$_{ax}$**. Overall, the effect of the additional ligand enhances the thermodynamical stability of the CC product relative to the CH product.

Our calculations reveal that the transition states are thermodynamically not stable with respect to dissociation of the PH₃ ligand (**TS-2-L**, R = methyl is not even a stationary point). A comparison of the reaction profiles with and without an additional ligand is given in Figure 9. The relative energies strongly suggest a dissociative reaction. In other words, reductive elimination and oxidative addition proceed from penta- to tetracoordinate species and conversely. A dissociative mechanism is also supported by previous experimental findings for reductive eliminations from Rh(III) complexes.[46] The coordination of an additional donor ligand occurs in a second step—
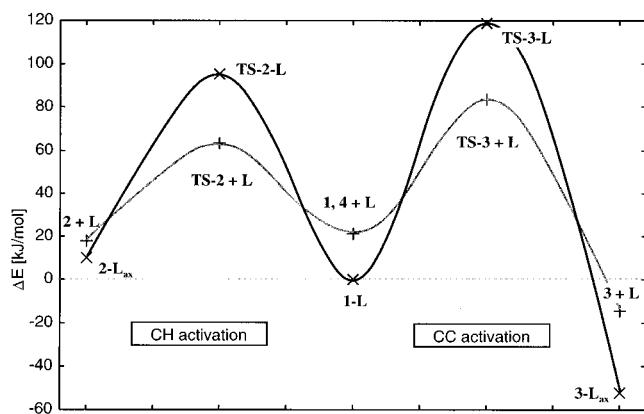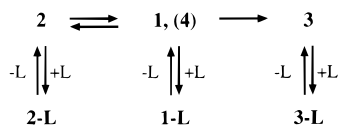
Figure 9. Comparison of the reaction profiles with and without a coordinated ligand (energies (ONIOM(B3LYP/lanl2dz:HF/lanl1mb)) relative to **1-L** for R = phenyl are plotted; for numerical data, see Table 10): ($\times$) PH$_3$ is coordinated; (+) PH$_3$ is not coordinated (the total electronic energy of PH$_3$ is just added to the curve in Figure 7).

Scheme 2

stabilizing the product complexes. Interestingly, the four-coordinate structure **1-L** is also very stable. In fact, it is even more stable than the CH product, but due to the very high activation barriers, it seems to be not accessible without prior dissociation of PH$_3$. Therefore, our calculations give evidence that the rate-determining step for the interconversion of the CH product into the CC product in the presence of a donor might be the dissociation of **1-L** into the intermediate complex **1** and the donor ligand **L**. So overall, the reaction in the presence of donor molecules should be described according to Scheme 2.

Conclusions

The results of our calculations may be summarized as follows:

CH and CC bond activation proceeds via a common intermediate structure in which the transition metal atom is close to the bonds to be cleaved.

The CC bond activation is in all cases thermodynamically favored over the CH bond activation. Our calculations give

evidence that this is a result of (a) the chelate core being less strained than in the CH product and (b) the reduced steric interaction of the chloro ligand with the substituents at the phosphorus atoms. For the reaction pathway we presented here, the activation barrier for CH activation is always substantially smaller. Therefore, CH bond cleavage is a reversible process.

In the case of electron-withdrawing substituents at the phosphorus atoms of the PCP ligand, activation barriers become higher.

Additional ligands coordinated to the rhodium atom enhance the stability of the CC insertion product over the CH insertion product. Instead of an agostic intermediate complex, a tetracoordinate species with no interaction of the transition metal atom with the methyl group of the PCP ligand has been found. A reaction pathway with a hexacoordinated rhodium atom in the transition state is unlikely. Our calculations predict a prior dissociation of the ligand.

The ONIOM model used in this study seems to be appropriate to obtain relative energies that are close to those from DFT calculations on the complete system. Experimentally determined structural parameters are well reproduced by the computational results. For future work it is interesting to investigate (a) the dependence on the transition metal and (b) the reaction profile for a PCN type ligand system[47] in which one phosphino (PR$_2$) group is replaced by an amino (NR$_2$) group. This work is currently in progress in our laboratory.

Supporting Information Available: Geometries in Cartesian coordinates for all species are available on the World Wide Web at the Uniform Resource Locator (URL) http://theochem. weizmann.ac.il/web/papers/Rh−CCvsCH.html. This material is available free of charge via the Internet at http://pubs.acs.org.

(46) Milstein, D. *Acc. Chem. Res.* **1984**, *17*, 221−226.

(47) Gandelman, M.; Vigalok, A.; Shimon, L. J. W.; Milstein, D. *Organometallics* **1997**, *16*, 3981−3986.

(48) Schaftenaar, G. Molden 3.6, 1999. URL: http://www.cmbi.kun.nl/∼schaft/molden/ molden.html.